Eco-Audit of MOFs as H_2 storage for Vehicle Applications, Using Novel Refueling Model

Elias Andraos and Guido Merino

Department of Chemistry, McGill University, 801 Sherbrooke Street West, Montreal, Quebec H3A 0B8, Canada

Abstract

Metal-organic frameworks (MOFs) are a heavily researched candidate for fuel-cell electric vehicle (FCEV) hydrogen storage. However, little analysis has been done of the environmental impact of potential MOF vehicles compared to established vehicles powered by renewable energy such as compressed hydrogen or battery-electric vehicles. In this work, a preliminary eco-audit of a FCEV using a hydrogen storage based on Ni_2(*m*-dobdc) (Ni-MOF-74), considering the cost and environmental impact of both production and use. The environmental impact of MOF production was compared to Li-ion battery production using both exergy calculations and embodied energy estimates. For the use phase, a hydrogen refueling station that produces hydrogen onsite by PEM electrolysis from grid electricity was compared to an equivalent population of BEVs charged at distributed recharging stations.

Introduction

Hydrogen has received much attention as a renewable vehicle fuel due to its high specific energy and potentially low footprint of production. The main challenge facing the application as a vehicle fuel is the low volumetric density of hydrogen. Current applications use either heavily compressed (350-700 bar) or cryogenic hydrogen, both of which come with a heavy energy penalty.[1] Even the theoretical minimum thermodynamic values for intense compression or liquefaction are a significant fraction of the specific energy of hydrogen (see Table 3), making possible alternatives to simple physical storage systems attractive. Chemical approaches to increase the energy density of hydrogen broadly fall into 4 categories; hydrogenation of organic molecules, synthesis of hydrogen-rich small molecules, metal hydrides, or adsorption.[2] Adsorption-based storage systems rely on the adsorption-desorption equilibrium lowering the gaseous pressure of H_2, increasing the possible volumetric density at lower pressures. Current candidates for adsorption-based hydrogen systems for fuel cell electric vehicles (FCEV) include graphene, multi-walled carbon nanotubes (MWCNTs), and metal-organic frameworks (MOFs).[3]

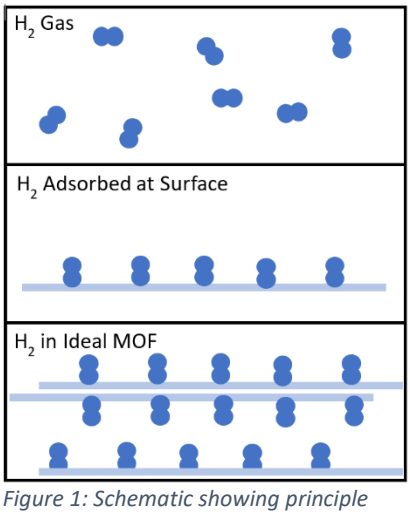

Figure 1: Schematic showing principle behind adsorptive H_2 storage.

MOFs

MOFs are a class of highly structured materials consisting of metal ions or clusters coordinated to organic linkages, also called secondary-building units (SBUs). The coordination geometry around the metal cluster as well as the shape of the organic link determine the 3D structure of the MOF. The long-scale order in MOFs makes them extremely porous, and the high variability in

the kind of cluster or linkage used allows for exact control of properties such as adsorption sites.[4] These properties combined make MOFs and attractive candidate for hydrogen storage via adsorption, as fine control over energies of adsorption and desorption in needed in order to provide both high H_2 bonding at high pressures as well as fast H_2 release at low pressures.[5]

Proposed Refueling Model

Due to the thermodynamic efficiency limits of hydrogen production by electrolysis and hydrogen oxidation by fuel cells, even an ideal hydrogen storage solution will not rival the cycle efficiency of a battery system.[6] An advantage of hydrogen as a fuel that may make up for this is that hydrogen can be stored between production by electrolysis and use in vehicles, compared to BEVs which must draw electricity from the grid while charging. In an electrical grid that has a significant share of renewable energy sources but relies on non-renewable energy instead of energy storage, as is the case for most current grids, CO_2 footprint and cost will vary significantly over timescales as short as hours. Being able to draw energy from the grid at a time when it is produced with a low carbon footprint and then storing it may lead to a lower overall footprint even if more electricity is used overall. Considering that most battery electric vehicles are charged overnight due to long charging times,[7] grids with an abundance of solar energy during the day may be an ideal target for such a FCEV refueling model.

Using MOF vehicle hydrogen storage is crucial to this model, as the lower operational pressures lower the energy requirements of hydrogen preparation. Additionally, current state-of-the-art refueling stations (for 350-700 bar vehicles) keep the majority of their hydrogen at a lower pressure in storage tanks before compressing it into short-term buffer tanks for use,[8] which must draw electricity at the time of demand instead of being able to wait for ideal conditions.

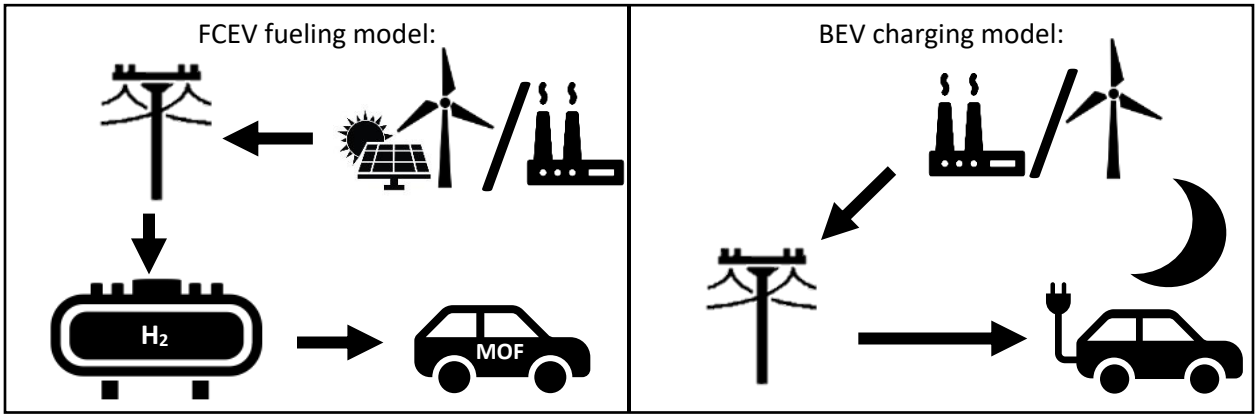

Figure 2: Proposed MOF-FCEV refueling model compared to model of current BEV charging.

Methods

Production Model

The production cost of a fuel cell electric vehicle with MOFs as hydrogen storage (MOF-FCEV) was estimated by the sum of literature and estimated production costs for the separate vehicle components constituting an MOF-FCEV. The production cost of the MOF material needed was modeled for the best current MOF[9] Ni_2(*m*-dobdc) by calculating the factor relating the Mg_2(dobdc) MOF cost[10] to the Mg_2(*m*-

dobdc) cost[11] and applying it to the Ni_2(dobdc) cost from literature.[10] This calculation was done considering two different synthesis methods for the MOF: liquid assisted grinding (LAG) and solvothermal. The total weight of MOF needed to adsorb the assumed 5.6 kg of H_2 for a full vehicle tank was determined by its reported 2.2 wt %.[10] The cost of a storage system using MOFs as hydrogen storage was previously modeled.[12] To incorporate the cost of the MOF material estimated in this report to the production cost of the storage system, the price for their estimated MOF material was replaced by the calculated total production cost of the required Ni_2(*m*-dobdc) to yield the total storage system cost. The hydrogen storage system must be attached to a fuel cell as to complete the power supply system of the MOF-FCEV. In this case, a proton exchange membrane (PEM) fuel cell of 80 kW for light duty vehicles was assumed to be the fuel cell of choice.[13] To complete the total production cost of a MOF-FCEV, an additional cost of $17,600 was assumed for other auto parts (including heating, ventilation, braking system, etc) along with appropriate mark-up percentages for the power supply production, marketing, warranty and profit costs from literature.[13] The calculated cost for the MOF-FCEV was compared to the production cost of a lithium ion battery electric vehicle (LIBEV) of same power as the MOF-FCEV fuel cell based on cost from Berckmans et al., 2017 (See Table 1).[14] Furthermore, the MOF-FCEV was compared to a FCEV for which the total cost was calculated following the same assumptions as the MOF-FCEV, where the cost of the MOF storage system was replaced with that for a type 4 compressed hydrogen storage system.[12]

Table 1: Key assumed values used for the calculation of the total cost of production of the various power supplies for electric vehicles

	Value	Unit
Production rate for vehicle components	500 000	Systems/year
PEM Fuel cell efficiency[15]	0.6	kWh/kWh
Electric vehicle efficiency[15]	0.3	kWh/km
PEM Fuel Cell cost rate for 80 kW low duty vehicle[13]	45	$USD/kW
mark up factor for power supply production[13]	1.17	
mark up factor for Marketing /warranty and profit[13]	1.29	
Lithium ion BEV cost of production (from NMC BEV)[14]	466	$/kWh

To assess the energetic impact of MOF-FCEV production, an estimation on the total embodied energy of production of a MOF-FCEV power supply (i.e: the MOF storage system and the PEM fuel cell) was conducted. The embodied energy of production for the MOF material was determined in two ways: by exergy approximation to attempt an estimate of the embodied energy for the specific best current MOF Ni_2(*m*-dobdc) and by utilizing literature values for a generalized MOF embodied energy.[16]

Exergy estimates the energy needed to produce a material by considering the maximum amount of work required to produce it as the minimum amount of work required to produce the material.[17] In other words, it assumes ideal values for the energy usage in production of a material. Furthermore, exergy calculations for materials assumes the exergy lost during a reaction to be equivalent to Gibbs energy of formation. The calculation needed to determine the total exergy of a material therefore involves summing the exergies of the elements it is comprised of and the Gibbs energy of formation, as seen in Equation 1.[17]

Equation 1: Exergy calculation for a material, where b is the exergy value, delta G is the Gibbs energy of formation, and 'c' and 'd' are the elements reacting to produce material 'cd'.

$$b_{cd} = b_c + b_d + \Delta G_{f,cd}$$

To use exergy as an approximation, the exergy of Lithium Cobalt Oxide (LCO) was calculated from literature values[18,19] and related to its literature embodied energy[20] by calculating a correlation factor. It was assumed that the synthesis methods for LCO (hydrothermal) and Ni-MOF-74 (Solvothermal) were comparable enough to offer an adequate comparison between embodied energies and exergies of material production. The calculated factor was applied to the exergy value calculated for Ni_2(*m*-dobdc) as to obtain the estimated embodied energy of its production. To calculate the total embodied energy of the power supply for a MOF-FCEV, the storage system required for MOF storage was assumed to be equivalent to that for a type 3 (350 bar) compressed hydrogen system as to readily obtain an estimate of hydrogen tank embodied energy by weight (see Table 2) and was summed to the material total embodied energy calculated. Furthermore, the embodied energy for production of the PEM fuel cell in the power supply system of the MOF-FCEV was calculated from 'case 3 of production' literature values (see Table 2), which assumes a mix in electricity grid composition going towards production of the PEM fuel cell and 75% recycling of the platinum group metals used in its production.[21]

This estimated total embodied energy of production was compared to a FCEV power supply made with the same PEM fuel cell as the MOF-FCEV power supply and with a type 4 (700 bar) compressed hydrogen storage system, for which embodied energy values can be seen in Table 2. It was also compared to a LCO BEV battery pack, for which the total embodied energy was calculated from its literature values (see Table 2).

Table 2: Key assumed values used for the calculation of the total embodied energy of various power supplies for electric vehicles

	Value	Units
Embodied energy for storage system (Type 3) production[22]	0.138	MJ/kg
Embodied Energy for a Type 4 (700 bar) hydrogen storage tank[22]	16.2	MJ/tank
case 3 estimated PEM embodied energy[21]	744	MJ/kW
LCO embodied energy[20]	320	MJ/kW
Li ion Battery production embodied energy (average)[23]	2318	MJ/kWh
Literature MOF Embodied energy[16]	91300	MJ/ton

Use Model

As shown in Figure 2, the model used is a refueling station that produces H_2 onsite by electrolysis during peak renewables capacity, stores it at 100 bar in traditional storage, until it is cooled to 198 K and filled into vehicle MOF tanks. On-site electrolysis capacity was modelled to be between 1500 and 2000 kW, falling well within a reasonable cost range for a refueling station using an estimate of $323/kW for mass-produced PEM-electrolyzers[24]. Energy for hydrogen compression and cooling was calculated using tabulated values[25], assuming ideal gas behavior of H_2, calculated values were compared to values from literature[1] to confirm that this assumption is reasonable in the range of conditions (see Table 1). H_2 demand modelled after USA gas station demand data from Nexant Inc. 2008[26] as reported in Grouset et al. 2018[27]. Battery vehicle charging demand was modelled after Fig 11. from Schey et al. 2012[7] (digitized using ImageJ). Station tank capacity was modelled after gas station underground tank sizes ranging from 12000-24000 gallons[28].

Quantity	Value	Unit
Ideal Energy of Isentropic Compression to 700 bar[1]	2.38	kWh/kgH_2
Real Energy of Compression to 700 bar[1]	2.72 - 7.42	kWh/kgH_2

Ideal Energy of H_2 Liquefaction[1]	3.9	kWh/kgH_2
Ideal Energy of Isothermal Compression to 700 bar[2]	2.25	kWh/kgH_2
Ideal Energy of Isothermal Compression to 100 bar[2]	1.58	kWh/kgH_2
Compressor Pump Efficiency[1]	92	%
Ideal Energy of Isobaric Cooling from 300 to 200 K [2]	0.41	kWh/kgH_2
Total Energy needed for H_2 Preparation before FCEV fueling[2]	2.13	kWh/kgH_2

Table 3: Thermodynamic Calculations for Preparation of H2 before FCEV fueling. 1) From Gardiner 2009 2) Own calculations, assuming ideal gas. All compression calculations assume H2 source at 1 bar.

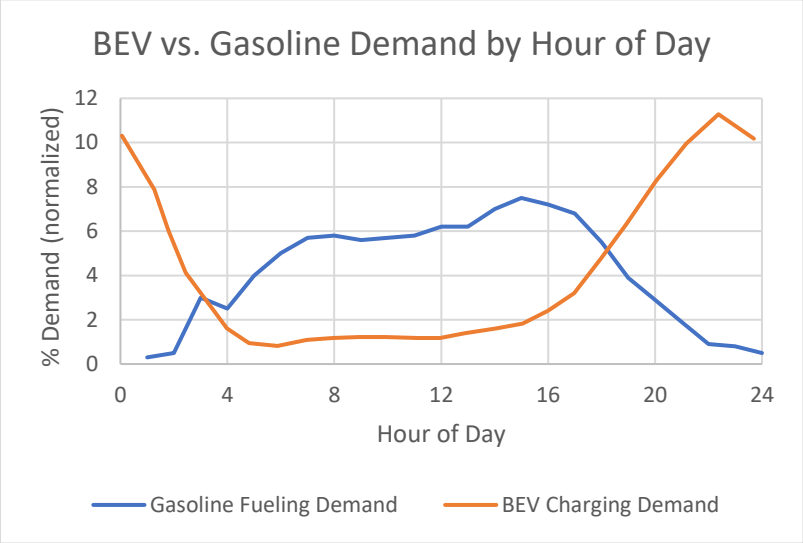

Figure 3: Demand models for BEV charging and gasoline refueling.

CO_2 footprint and cost of electricity use were compared using best- and worst-case numbers for different electricity sources.[29] CO_2 footprint per kWh was calculated according to Equation 2. Cost per kWh was calculated using estimates for delivered cost of individual electricity types, as actual pricing schemes varied between Ontario and California, and varied by type of consumer.

Equation 2: Total CO_2 intensity as calculated from values in Information Pack.

$$Total\ CO_2\ intensity\ \left(\frac{kg}{kWh}\right) = CO_2\ int.fuel\ \left(\frac{kg}{kWh}\right) + \frac{CO_2\ int.construction\ (\frac{kg}{kW})}{plant\ lifespan\ (h) * capacity\ factor}$$

Geothermal energy was excluded as no estimate for delivered cost was included in the data set. Because hourly averages of the composition of the power grid lose information about intermittent power sources such as wind (see Figure 4), the model calculated the energy used hour-by-hour over one year using data from 2019 from Ontario[30] and California[31]. California is a prime example of an electrical grid with a large percentage of renewables but without adequate grid storage, resulting in a large difference

in CO2 footprint across the day. Ontario was chosen as a reference for a more diverse grid, with significant contribution from low-impact nuclear and hydro sources (see SI for raw grid composition data).

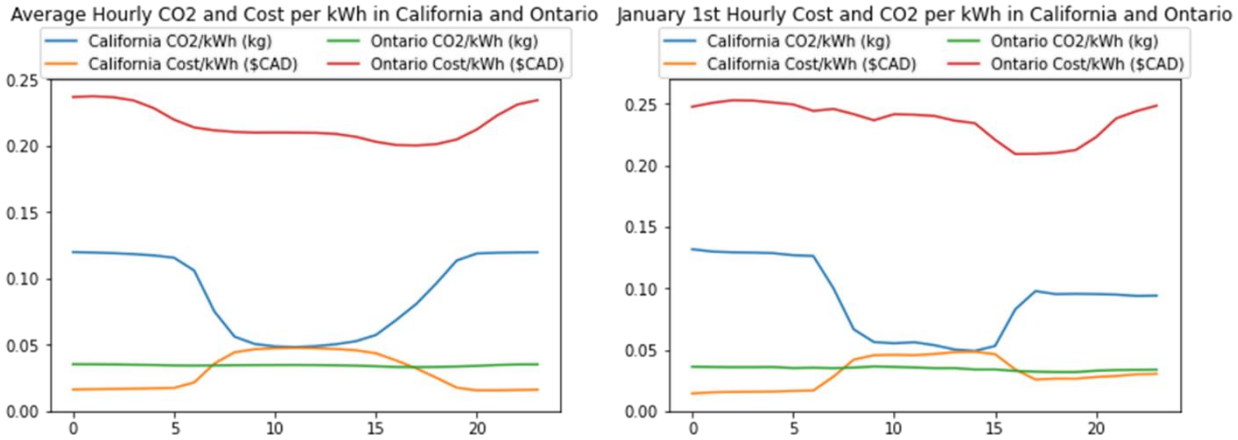

Figure 4: Plots showing CO2 footprint and cost per kWh of grid electricity in California and Ontario, a) averaged over 2019 and b) for January 1st. Other days showed even larger difference, but Jan. 1st was chosen for transparency. Differences show that simply considering hourly averages is too reductive, as renewable energy sources are not regular, especially in the case of wind energy in Ontario.

The model used to represent the refueling station optimizing its electricity use was fairly simple, electricity was drawn from the grid to produce hydrogen if the hourly carbon footprint was lower than the average of the twelve hours before and after. Of course, a real refueling station would not have exact grid composition data available for the future, but weather forecasts should be able to provide a fairly good estimate of the amount of wind and solar energy that might be available within 12 hours. Additionally, electricity would be used at sub-optimal hours if the station tank reached a minimum threshold. Better performance could be achieved with larger electrolyser capacity used over a shorter time every day, but this cost-benefit analysis is outside of the scope of this project. Optimization of cost was also considered but losses in carbon footprint made this option unattractive (see model in SI).

Results - Eco-Audit

Production – Cost & Embodied Energy comparison

Given the assumptions made, the results show the financial advantage of production of a MOF-FCEV. As seen in Figure 5, the total cost of production for an electric vehicle using the best current MOF as hydrogen storage is lower than that for a lithium ion battery electric vehicle, but remains higher than the production cost of a fuel cell electric vehicle with a compressed hydrogen storage system. However, development of an MOF which would have higher hydrogen capacity per volume could lower those costs by reducing the amount of MOF mass and offer a competitive alternative to power supply for fuel cell electric vehicles.

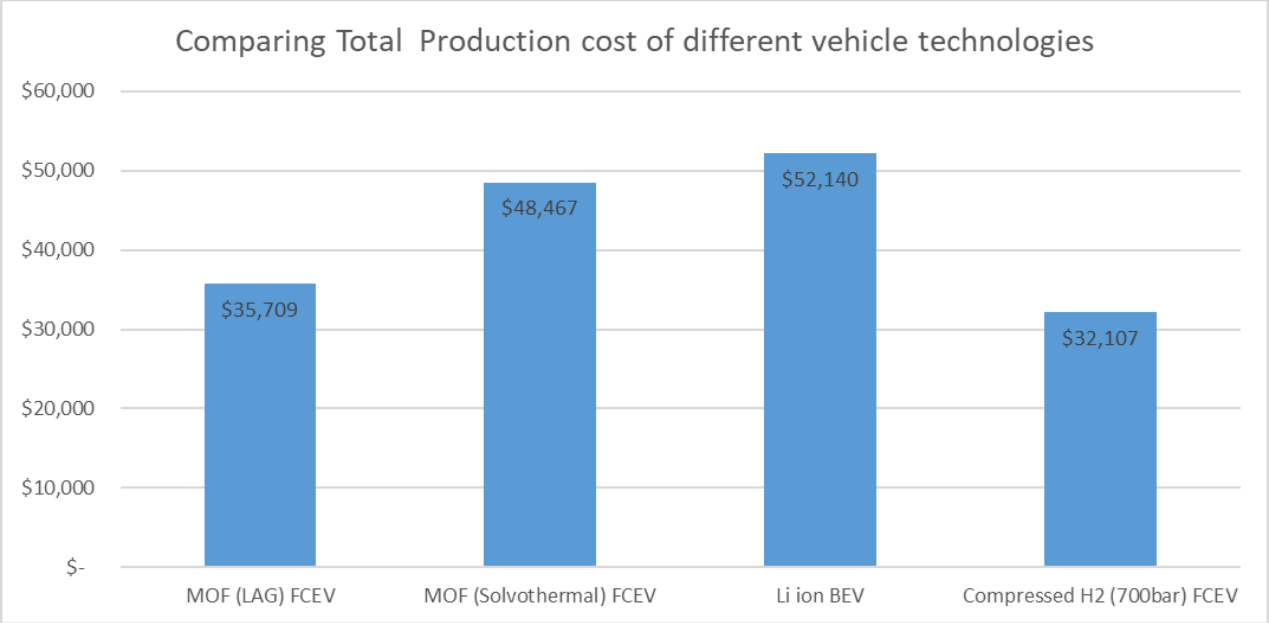

Figure 5: Comparison of the resulting total cost (in $USD) of vehicle production for different power supply methods and synthesis methods of MOF material.

The total cost of a MOF-FCEV also depends on the synthesis method employed. The most widely used to date for MOF synthesis in MOF research and development is Solvothermal synthesis. As seen from Figure 6, the cost of MOF material production greatly increases due to the synthesis requiring expensive organic solvents to dissolve the materials. By modifying the synthesis method to liquid assisted grinding, it was found in literature and clearly demonstrated below that the cost of production greatly lowers due to no organic solvent being used.[10] This further confirms the potential of MOF hydrogen storage systems as a competitor for compressed hydrogen fuel cell vehicles since the development of better MOFs and MOF synthesis could further reduce the production costs.

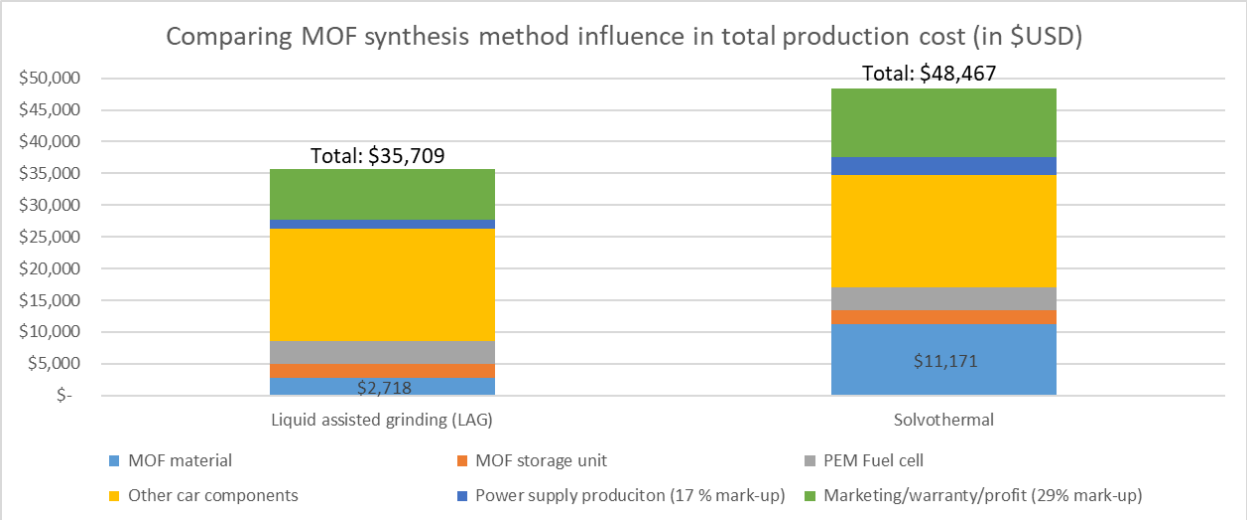

Figure 6: Comparison of the total production costs for two different synthesis methods of the MOF.

The estimated embodied energy of 13582 MJ/kg for the Ni_2(*m*-dobdc) MOF production calculated by exergy was discarded for further comparison as it is around 10 times greater than the reported literature embodied energy of 101 MJ/kg for a general MOF. The results using the latter embodied energy for MOF material were therefore compared to other power supply technologies for electric vehicles to assess the energetic impact of producing an MOF storage system. As seen in Figure 7 below, the MOF storage system production shows promising results for its integration as a power supply for electric vehicles with a roughly three times lower embodied energy requirement for production to that of a LCO battery electric vehicle.

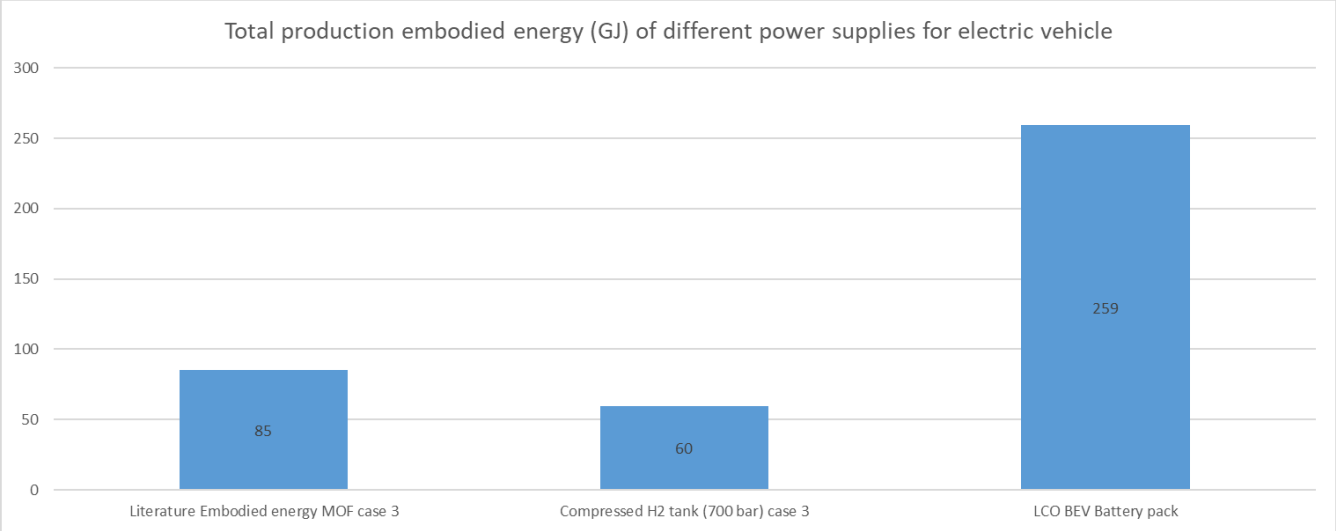

Figure 7: Comparison of the total embodied energy of production of electric vehicles with different power supplies, where the embodied energy for material production for the MOF case was from literature and case 3 denotes the conditions of PEM FC production previously stated.

Similarly to the cost of production results, there is still some modifications to do to the MOF storage which can be undertaken to allow for competition with the hydrogen compressed storage fuel cell electric vehicles. As seen from Figure 8, the MOF material contributes to 30% of the total embodied energy of production. As previously mentioned, the development of a better MOF which would reduce the total mass of the MOF material would offer competitiveness.

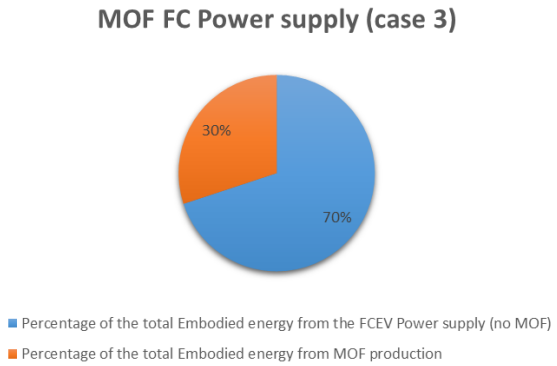

Figure 8: Percentage contribution to the total embodied energy of the fuel cell vehicle power supply by the MOF material.

Use Phase

The results of refueling model described in the Methods section above are shown in Figure 9. In the solar-dominated Californian grid, MOF-FCEVs can achieve similar carbon footprint values to BEVs, albeit at higher cost (this is discussed in Limitations below). In Ontario the fluctuation of renewables, mainly wind, is not enough to make up for the lower efficiency of FCEVs, and both the carbon footprint and price show this.

From the cost estimate for the production of an MOF-FCEV compared to a BEV and the estimated cost per kilometer driven, a break-even point of 960,000-740,000 km in California or 310,000 to 150,000 km in Ontario for the LAG-MOF vehicle compared to the BEV vehicle can be calculated. No lifespan data is available for MOFs for hydrogen storage, but the break-even point for California is well outside of the lifespan of a battery or fuel-cell, while the Ontario point is approximately equal to or just beyond the lifespan of a battery for a BEV.

Comparing the environmental impacts of both the production and use of an MOF-FCEV compared to a BEV would require additional information, as embodied energy does not translate directly to greenhouse gas emissions. However, it is safe to say that MOFs are roughly comparable to BEVs in both production and use phases in terms of cost and environmental footprint.

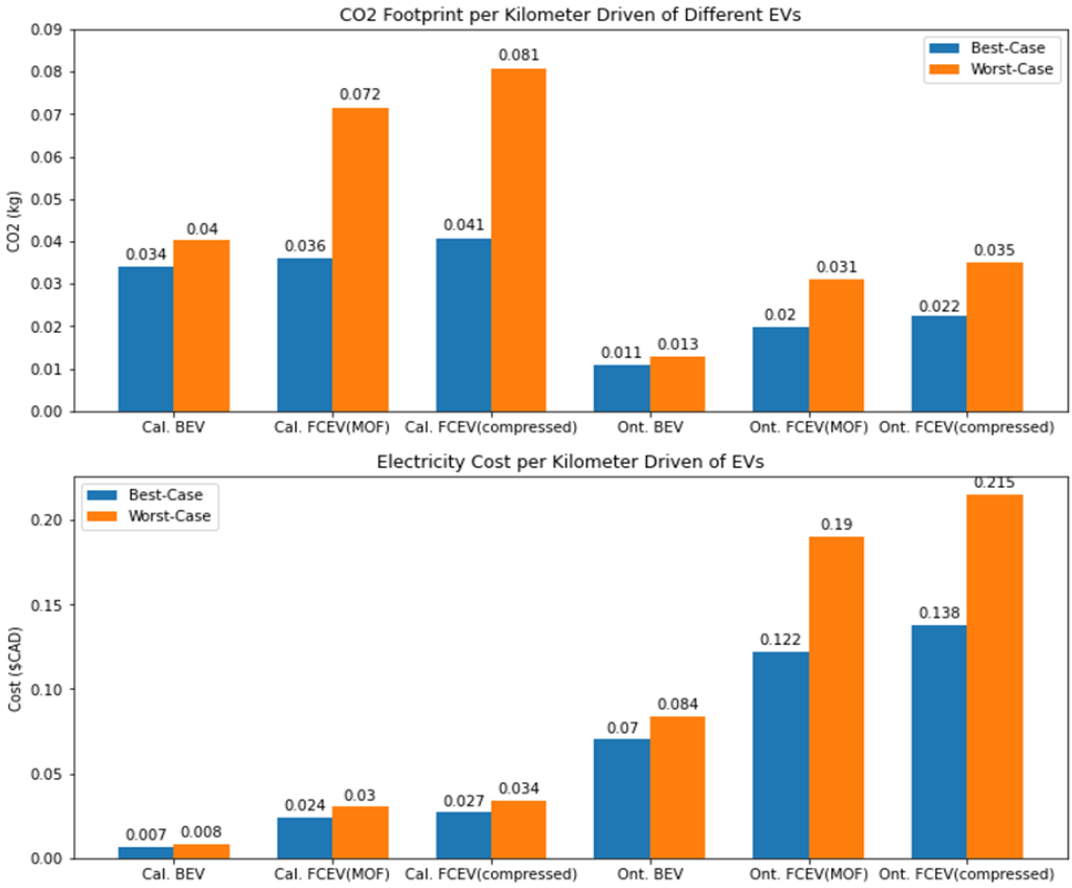

Figure 9: Results of refueling model. FCEV using 700 bar compressed system was added for comparison, by scaling MOF-FCEV values by factor shown in Table 3. Compressed-H_2 FCEV values are likely underestimated due to the model being tailored towards MOF-FCEVs.

Conclusions

Potential

We believe our estimates and preliminary calculations show that MOF hydrogen storage systems have the potential to compete with battery systems for vehicle energy storage, both in terms of CO_2 footprint and in terms of cost. Despite the rough estimates made due to lack of data, our modelling approach can be easily refined when more data becomes available. The MOF considered for this model, Ni_2(*m*-dobdc), is an already synthesized material, other MOFs that may be better suited for H2 storage have already been identified in theoretical work.[32]

One technology that may also greatly improve the competitiveness of MOF-FCEVs and FCEVs in general is high-pressure electrolysis, which might produce hydrogen at pressures high enough for direct use, eliminating the need for compression.[33] MOF-FCEVs might benefit more from this technology than other FCEVs due to lower pressure requirements.

Limitations

As stated previously, fairly rough estimates had to be made for multiple values due to a lack of available data.

Production phase: No real embodied energy available, must determine it and find one with low embodied energy to produce MOF material.

The difference in vehicle space and weight requirements were not considered, even though they are significant. Despite the mass density of only 2.2% H_2 in the MOF, the total mass needed for hydrogen storage ranges from 175 to 205 kg, while the BEV requires between 965 and 1265 kg of batteries. The volume occupied by the energy storage is also markedly better for the MOF-FCEV, with only about 0.2 m^3 needed compared to 0.5 to 1.2 m^3 for a BEV. While neither of these values for the MOF-FCEV include the fuel cell, the difference is large enough to show the advantage of an MOF hydrogen storage system over batteries for vehicle design. Despite these differences, both types of vehicles were modelled as having an efficiency of 0.3 kWh/km.[15] Accounting for this difference may significantly improve the results of the MOF-FCEV.

As mentioned above, no degradation data or estimates are available for MOF hydrogen storage systems, so the fuel cell was taken to be the limiting factor in terms of vehicle lifespan. No end-of-life recovery was considered. Li-ion battery recycling is challenging but under development, while no data on MOF recycling was found.

References

(1) Gardiner, M. Energy Requirements for Hydrogen Gas Compression and Liquefaction as Related to Vehicle Storage Needs. US Department of Energy October 26, 2009.

(2) Hydrogen Storage https://www.energy.gov/eere/fuelcells/hydrogen-storage (accessed Nov 24, 2020).

(3) Gangu, K. K.; Maddila, S.; Mukkamala, S. B.; Jonnalagadda, S. B. Characteristics of MOF, MWCNT and Graphene Containing Materials for Hydrogen Storage: A Review. *J. Energy Chem.* **2019**, *30*, 132–144. https://doi.org/10.1016/j.jechem.2018.04.012.

(4) Gangu, K. K.; Maddila, S.; Mukkamala, S. B.; Jonnalagadda, S. B. A Review on Contemporary Metal–Organic Framework Materials. *Inorganica Chim. Acta* **2016**, *446*, 61–74. https://doi.org/10.1016/j.ica.2016.02.062.
(5) Langmi, H. W.; Ren, J.; Musyoka, N. M. 7 - Metal–Organic Frameworks for Hydrogen Storage. In *Compendium of Hydrogen Energy*; Gupta, R. B., Basile, A., Veziroğlu, T. N., Eds.; Woodhead Publishing Series in Energy; Woodhead Publishing, 2016; pp 163–188. https://doi.org/10.1016/B978-1-78242-362-1.00007-9.
(6) Haseli, Y. Maximum Conversion Efficiency of Hydrogen Fuel Cells. *Int. J. Hydrog. Energy* **2018**, *43* (18), 9015–9021. https://doi.org/10.1016/j.ijhydene.2018.03.076.
(7) Schey, S.; Scoffield, D.; Smart, J. A First Look at the Impact of Electric Vehicle Charging on the Electric Grid in The EV Project. *World Electr. Veh. J.* **2012**, *5* (3), 667–678. https://doi.org/10.3390/wevj5030667.
(8) Reddi, K.; Elgowainy, A.; Rustagi, N.; Gupta, E. Two-Tier Pressure Consolidation Operation Method for Hydrogen Refueling Station Cost Reduction. *Int. J. Hydrog. Energy* **2018**, *43* (5), 2919–2929. https://doi.org/10.1016/j.ijhydene.2017.12.125.
(9) Kapelewski, M. T.; Runčevski, T.; Tarver, J. D.; Jiang, H. Z. H.; Hurst, K. E.; Parilla, P. A.; Ayala, A.; Gennett, T.; FitzGerald, S. A.; Brown, C. M.; Long, J. R. Record High Hydrogen Storage Capacity in the Metal–Organic Framework Ni2(m-Dobdc) at Near-Ambient Temperatures. *Chem. Mater.* **2018**, *30* (22), 8179–8189. https://doi.org/10.1021/acs.chemmater.8b03276.
(10) DeSantis, D.; Mason, J. A.; James, B. D.; Houchins, C.; Long, J. R.; Veenstra, M. Techno-Economic Analysis of Metal–Organic Frameworks for Hydrogen and Natural Gas Storage. *Energy Fuels* **2017**, *31* (2), 2024–2032. https://doi.org/10.1021/acs.energyfuels.6b02510.
(11) Houchins, C.; James, B. *Hydrogen Storage System Cost Analysis: Summary of FY 2017 Activities Sponsorship and Acknowledgements*; 2017. https://doi.org/10.13140/RG.2.2.34567.85927.
(12) James, B. D.; Houchins, C.; Huya-Kouadio, J. M.; DeSantis, D. A. *Final Report: Hydrogen Storage System Cost Analysis*; DOE-SA-0005253; Strategic Analysis Inc., Arlington, VA (United States), 2016. https://doi.org/10.2172/1343975.
(13) James, B. D.; Huya-Kouadio, J. M.; Houchins, C.; DeSantis, D. A. V.E.5 Fuel Cell Vehicle Cost Analysis. *Strateg. Anal.* **2017**, 6.
(14) Berckmans, G.; Messagie, M.; Smekens, J.; Omar, N.; Vanhaverbeke, L.; Van Mierlo, J. Cost Projection of State of the Art Lithium-Ion Batteries for Electric Vehicles Up to 2030. *Energies* **2017**, *10* (9), 1314. https://doi.org/10.3390/en10091314.
(15) McCalla, E. L11-FC-Performance - Fall 2020 - CHEM-429-001 - Chem of Energy, Storage & Util. 2020.
(16) Sathre, R.; Masanet, E. Prospective Life-Cycle Modeling of a Carbon Capture and Storage System Using Metal–Organic Frameworks for CO2 Capture. *RSC Adv.* **2013**, *3* (15), 4964–4975. https://doi.org/10.1039/C3RA40265G.
(17) McCalla, E. L4-Exergy - Fall 2020 - CHEM-429-001 - Chem of Energy, Storage & Util. 2020.
(18) De Meester, B.; Dewulf, J.; Janssens, A.; Van Langenhove, H. An Improved Calculation of the Exergy of Natural Resources for Exergetic Life Cycle Assessment (ELCA). *Environ. Sci. Technol.* **2006**, *40* (21), 6844–6851. https://doi.org/10.1021/es060167d.
(19) Jain, A.; Ong, S. P.; Hautier, G.; Chen, W.; Richards, W. D.; Dacek, S.; Cholia, S.; Gunter, D.; Skinner, D.; Ceder, G.; Persson, K. A. Commentary: The Materials Project: A Materials Genome Approach to Accelerating Materials Innovation. *APL Mater.* **2013**, *1* (1), 011002. https://doi.org/10.1063/1.4812323.
(20) Dunn, J. B.; Gaines, L.; Kelly, J. C.; Gallagher, K. G. Life Cycle Analysis Summary for Automotive Lithium-Ion Battery Production and Recycling. In *REWAS 2016: Towards Materials Resource Sustainability*; Kirchain, R. E., Blanpain, B., Meskers, C., Olivetti, E., Apelian, D., Howarter, J.,

Kvithyld, A., Mishra, B., Neelameggham, N. R., Spangenberger, J., Eds.; Springer International Publishing: Cham, 2016; pp 73–79. https://doi.org/10.1007/978-3-319-48768-7_11.
(21) Pehnt, M. Life-Cycle Assessment of Fuel Cell Stacks. *Int. J. Hydrog. Energy* **2001**, *26* (1), 91–101. https://doi.org/10.1016/S0360-3199(00)00053-7.
(22) Evangelisti, S.; Tagliaferri, C.; Brett, D. J. L.; Lettieri, P. Life Cycle Assessment of a Polymer Electrolyte Membrane Fuel Cell System for Passenger Vehicles. *J. Clean. Prod.* **2017**, *142*, 4339–4355. https://doi.org/10.1016/j.jclepro.2016.11.159.
(23) Ellingsen, L. A.-W.; Majeau-Bettez, G.; Singh, B.; Srivastava, A. K.; Valøen, L. O.; Strømman, A. H. Life Cycle Assessment of a Lithium-Ion Battery Vehicle Pack. *J. Ind. Ecol.* **2014**, *18* (1), 113–124. https://doi.org/10.1111/jiec.12072.
(24) Shiva Kumar, S.; Himabindu, V. Hydrogen Production by PEM Water Electrolysis – A Review. *Mater. Sci. Energy Technol.* **2019**, *2* (3), 442–454. https://doi.org/10.1016/j.mset.2019.03.002.
(25) McCarty, R. D.; Roder, H. M.; Hord, J.; Center for Chemical Engineering (U.S.); United States. *Selected Properties of Hydrogen (Engineering Design Data)*; NBS monograph ;168; U.S. Dept. of Commerce, National Bureau of Standards : For sale by the Supt. of Docs., U.S. G.P.O.: Washington, D.C., 1981.
(26) Nexant, I. H2A Hydrogen Delivery Infrastructure Analysis Models and Conventional Pathway Options Analysis Results. **2008**.
(27) Grouset, D.; Ridart, C. Chapter 6 - Lowering Energy Spending Together With Compression, Storage, and Transportation Costs for Hydrogen Distribution in the Early Market. In *Hydrogen Supply Chains*; Azzaro-Pantel, C., Ed.; Academic Press, 2018; pp 207–270. https://doi.org/10.1016/B978-0-12-811197-0.00006-3.
(28) How Much Gas Does a Tanker Truck Hold? *Transcourt Inc.*, 2018.
(29) McCalla, E. L7-Information-Pack - Fall 2020 - CHEM-429-001 - Chem of Energy, Storage & Util. 2020.
(30) Ontario Independent Electricity System Operator. Generator Output by Fuel Type Hourly Report https://www.ieso.ca/Power-Data/Data-Directory.
(31) California Independent System Operator. Daily Renewables Output Data http://content.caiso.com/green/renewrpt/20181231_DailyRenewablesWatch.txt (accessed Nov 14, 2020).
(32) Ahmed, A.; Seth, S.; Purewal, J.; Wong-Foy, A. G.; Veenstra, M.; Matzger, A. J.; Siegel, D. J. Exceptional Hydrogen Storage Achieved by Screening Nearly Half a Million Metal-Organic Frameworks. *Nat. Commun.* **2019**, *10* (1), 1568. https://doi.org/10.1038/s41467-019-09365-w.
(33) Marangio, F.; Santarelli, M.; Calì, M. Theoretical Model and Experimental Analysis of a High Pressure PEM Water Electrolyser for Hydrogen Production. *Int. J. Hydrog. Energy* **2009**, *34* (3), 1143–1158. https://doi.org/10.1016/j.ijhydene.2008.11.083.

Software Used

Calculations and Figures: Excel, Jupyter Notebook

Image digitization: ImageJ

Image Credits:

Figure 2: Built-in Word icons, Andrejs Kirma from the Noun Project